

## The Role of Fabricated Coral Shell Hydroxyapatite Powder in the Healing of Large Size Mandibular Bone Gap Defect in Dogs

Ali Ghazi Atiyah<sup>1</sup>, Alkattan Layth Mahmoud<sup>\*2</sup>

<sup>1</sup>Department of Surgery and obstetric, College of Veterinary Medicine, University of Tikrit, Tikrit, Iraq.

<sup>2</sup>Department of Surgery and Theriogenology, College of Veterinary Medicine, University of Mosul, Mosul, Iraq.

### Abstract

**BAGROUND :** The reconstruction of mandibular bone defect comprised a real challenge and difficult task for surgeons, biomaterial bone substitutes are the most used material for reconstruction mandibular bone defect.

**OBJECTIVES:** This study explored the role of fabricated Hydroxyapatite (HAp) powder from the coral shell in healing critical size mandibles gap in dogs.

**METHODS:** HAp was prepared by hydrothermal method from Coral shells. Characterization of the fabricated coral shell was done by X-ray diffraction (**XRD**), Field emission scanning electron microscopy (**FESEM**), and Energy dispersive X-ray spectroscopy(**EDX**). The designed research was performed on eighteen dogs of both sexes weighted and aged ( $20 \pm 0.5$  kg), ( $2 \pm 0.6$  years). The experiment was divided into two equal groups. Animals underwent experimental defects at the ventral surface of the lower mandible about (14, 5 mm).

**RESULTS:**The results of (XRD) represented high crystallinity, the (EDX) results indicated the surface morphology of distributed particles of calcium, phosphor, carbon, and oxygen, respectively, and the FESEM results suggested that the surface morphology of (HAp) appears as a spherical particle that regularly distributed within the sample. In the (HAp)group, at 30 days, the FESEM images show that the defective gap completely closed, and the center of the defect was filled with a thick layer of osteoid matrix. Radiographically in (HAp) group at 30 days post-surgery indicated a well-defined circular radiolucent bone gap at the caudal portion of the mandible, with a partially sclerosed margin. Macroscopically at 30 days, the gap appears very small in size, invaded with new bone formation.

**CONCLUSION:** In conclusion, the recycling (HAp) from coral shells has practical value in the reconstitution of the mandibular gap and the radiological and critical properties of prepared (HAp) emphasize this outcome.

**Keywords:** Bone gap, Bone healing, Coral shell, Large size, Mandible.

## Introduction

Biomaterial bone substitutes are the most used material for the reconstruction of bone defects regarding biochemical properties, availability, and simplified and low fabrication cost (Shafiei et al., 2012). These materials are commonly used in the orthopedic field as a mandibular defect that comprises the essential affections in maxillofacial bone fracture or discontinuity of the mandible in case of loss of a portion of the lower mandible (Lim et al., 2022). Therefore, the reconstruction of mandibular bone defect comprised a real challenge and difficult task for surgeons to the lower jaw's inferior aesthetic point and functional properties (Paré et al., 2019). Hydroxyapatite is an inorganic component constituting the bone with the formula  $\text{Ca}_{10}(\text{PO}_4)_6(\text{OH})_2$ . It's used as a bone substitute bioactive material due to its osteoconductive biocompatible and nontoxic properties (Szczęs et al., 2017) and used as bone filler. (HAp) has the same bone composition, are highly biocompatible, and stimulate bone growth (Albaroudy et al., 2022 ; Allawi et al., 2020 ). It is inert immunologically and does not provoke highly sensitive reactions due to the high-heat method used to produce this compound (Cahyaningrum, et al., 2018). Recently, bone substitutes biomaterials from synthetic or natural sources used for treatment of critical size bone defect that have a similar structure to the inorganic bone phase appeared as an alternative to metallic grafts and fabricated to make

chemical bonds with the bone and have the ability to reconstruct bone defects ( Pina et al., 2018; Anvar et al., 2022). Coralline materials and eggshells, considered natural sources of apatite ceramic, can be used as filling materials in orthopedic surgery, in which the chemical structure is closely similar to the inorganic phase of the living bones and teeth (Khan et al., 2019; Zhang et al., 2019). Also, hydroxyapatite nanoparticles are applied as bone substitute bioactive material it improves the regeneration of the vertical bone model (Kaneko et al., 2020). Many studies suggested that the apatite materials' ionic and mineral elements rapidly incorporate enhanced biocompatibility and provide physicochemical reactions that can accelerate the bone formation and regeneration (Atiyah, et al., 2021; Pina et al., 2010; Yal Beiranvand et al., 2022) . The absence of a well-documented large size bone gap defect in the dog mandible that experimentally treated with coral shell hydroxyapatite powder makes experimental results questionable, so this study suggested to determine the effects of prepared coral shell (HAp) powder in healing of the large-size of mandibles bone gap defects in the dog model.

## **Materials and Methods**

This experiment was approved by the institutional animal care and use committee at the College of Veterinary Medicine, Mosul University No. (UM.VET.2022.050). In the current experimental study, eighteen clinically healthy adult local breed dogs of both sexes with a weight of  $(20 \pm 0.5)$  kg and age were  $(2 \pm 0.6)$  years were used. All experimental animals were clinically

inspected for any infectious disease. All animals were housed at the animal house of Veterinary Medicine College, At the University of Mosul, along the period of the experiment.

### **Laboratory preparation of coral shell hydroxyapatite powder:**

The coral shells (Pectinidae) were purchased from the local market in Basra City, Iraq, then washed using distilled water. Later, the shells were boiled in a mixture of distilled water and ethanol to remove any organic residues, then dried in the oven at 100 °C for 30 hour. The dried shells were then grounded to a fine powder using an electrical mortar grinder (Retsch, RM200, China). The powder was calcined in a muffled furnace (Prothrom- Turkey) at 1200 °C for 2 hours to produce calcium hydroxide powder. Later, an orthophosphoric acid solution (Ridel-Turkey) with 0.6 M was added to the Ca(OH)<sub>2</sub> solution to justify the pH of the solution at (8.5) using a pH meter (AD1000-Germany). The white homogenous precipitate was observed at this point. The product was kept at ambient temperature for 48 hours in order to aging, which allowed the complete chemical reaction. The dried precipitation was calcined at 1200 °C for 2 hours in a muffled furnace. The white crystalline powder was produced. (Fig. 1), indicated the presence of (HAp) white crystal powder. Chemical equations are mentioned below:

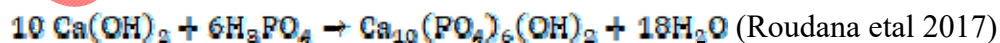
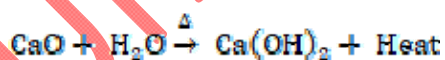




Figure (1): fabricated coral shell hydroxyapatite powder

### **Characterization of fabricated coral shell (HAp) Powder**

#### **X-ray diffractometer (XRD) analysis**

The X-ray diffraction (XRD) analyses were performed to determine the crystal phase and purity of coral shell HA. powders samples. The XRD data were recorded within the two theta ( $2\theta$ ) range from zero<sup>0</sup> to 80<sup>0</sup>, and intensity counts range from zero to 900<sup>0</sup>, used (Malvern Panalytical, Aeris, UK).

#### **Field emission scanning electron microscopy (FESEM)**

The surface morphology, crystal size, and porosity of the fabricated coral shell (HAp) powder were detected by the field emission scanning electron microscope (FESEM) model (inspect f 50, fei, Holland). Also, the FESEM image was taken 30 days post-surgery. All samples were subjected to gold covering before electron microscopy to give the necessary conductivity.

### **Energy dispersive X-ray spectroscopy (EDX)**

The EDX analysis determined the elemental compositions and the relative concentrations of the main trace elements, such as calcium, phosphor, and oxygen, of the fabricated coral shell (HAp) powder samples. It also used to determine the elements distribution mapping to reveal the surface topography of these elements through an energy dispersive X-ray microanalysis system model (inspect f 50, Fei, Holland) with an acceleration energy voltage range from zero to 20 keV. This technique done in labs of ministry of science and technology, Baghdad ( Tatara et al., 2019; Atiyah et al.,2022)

The experimental animals were randomly divided into two equal experimental groups (n=9):

Group 1: control group, a circular mandibular bone gap defect of (14 ×5) mm. in diameter was created in the caudal portion of the mandible used a low-speed bone drill under continuous irrigation with 0.9% sterile saline solution and left empty without any treatment.

Group 2: treated group, the same mandibular bone gap defects were created and then filled with 5 gm of previously fabricated coral shell hydroxyapatite (HAp) powder.

### **Surgical procedure.**

All operative dogs underwent a protocol of general anesthesia, including a combination of 10 % ketamine HCL (Alfasan, Holland) and 2% xylazine (Interchemie, Holland) at a dose (10mg/kg) and (5 mg/kg), respectively, through intramuscular injection (Greene and

Thurmon,1988;Alkattan and Helal,2013). The operative region was aseptically prepared, skin incision approximately (4 cm) in length was performed along the ventral part of the lower mandible in (the submandibular region) followed by blunt dissection of platysma muscles to expose the mandibular bone (Fig. 2,A). To create a critical-sized mandibular bone defect in a sagittal incision of approximately (14×5) mm. in diameter was made in all groups of the animal, without perforation of the underlying buccal mucosa, using a slow-speed bone drill combined with a diamond hole saw (Juster, j3901, China) with continuous irrigation with 0.9%saline solution to prevent heat damage to the bone tissue to form a circular defect gap (Fig. 2,B). In the control group, the defective gap was left empty without any treatment in the control group (Fig. 2,C). The defect gap in the treated group was filled with fabricated coral shell (HAp) powder (Fig. 2,D).

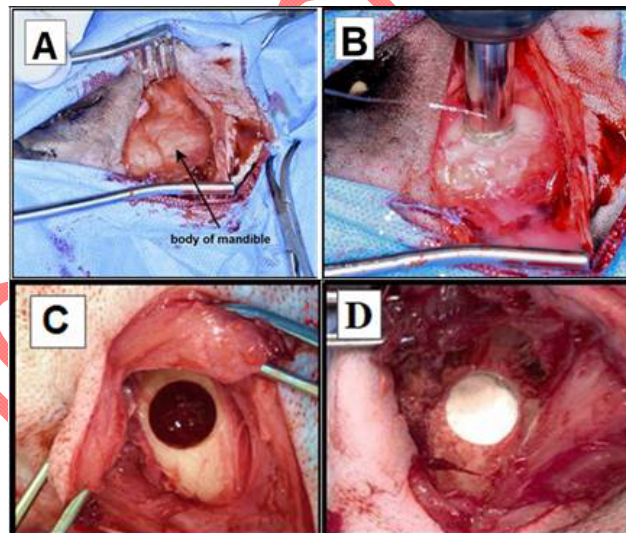


Figure (2): (A) surgical approach to the body of the mandible. (B) creation of circular mandibular bone gap defect (C) The control group, (D) The treated group, the defect gap was filled with coral shell (HAp) Powder.

### **Macroscopical evaluations**

The site of operation evaluated macroscopically in the control and treated group at 7, 15 and 30 days post-surgery to observe the gross findings within the site of the mandibular bone gap and to inspect any changes that may be existed.

### **Radiographical evaluations**

The lateral view of the skull was taken immediately after surgery and then at (15,30,60) intervals days post-surgery, using an X-ray machine (Shimadzu, Japan) accompanied by the digital wireless detector (Italray, Italia) with exposure factors seated as 65 kV and 2.5 mAs, to investigated of the position and the density of the bone gap, the presence of periosteal reaction, new bone formation.

## **Results**

### **Characterization of fabricated coral shell HAp.**

**X-Ray Diffraction:** The results of XRD patterns of the fabricated coral shell HA. Powder sample revealed that the typical intense peaks were detected with high crystallinity at  $2\theta$  (25.46°, 28.85°, 31.74°, 32.75°, 39.80°, 46.44°, 49.11°, 52.98°, 76.51°) respectively associated with the hexagonal crystalline shape of calcium hydroxide. All these peaks were in agreement with the

international center for diffraction data (ICDD), card number (09-0432) used Qualx software version 2.25. (Fig. 3).

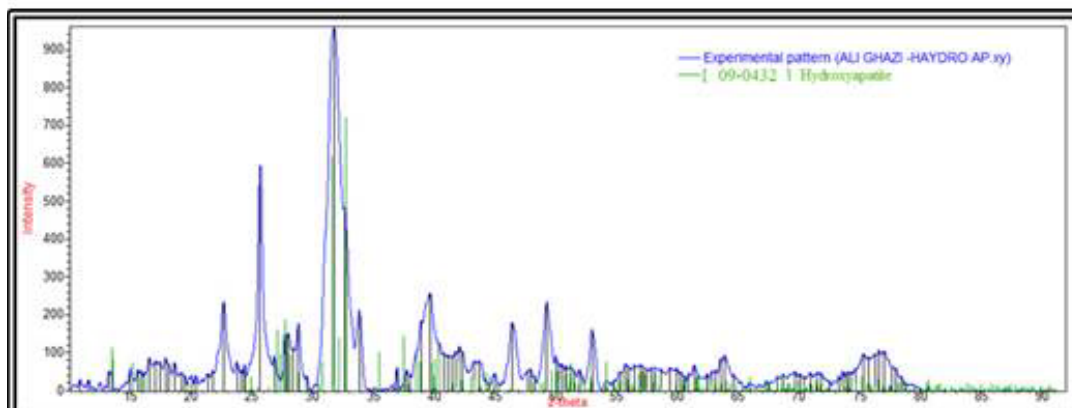


Figure (3): XRD diffraction peaks of the fabricated coral shell (HAp) heated at 1200°C for 2 h. at 2θ range from zero-90 degree and intensity range from zero- 1000

**Energy Dispersive X-ray spectroscopy (EDX):** The EDX spectrum of the fabricated coral shell (HAp) powder, shown in Figure (4), reveals the presence of calcium (Ca), phosphor (P), oxygen (O), carbon (C) and potassium (K). Quantity values measured in atomic and weight % were listed in Table (1). The EDX elemental mapping of fabricated coral shell (HAp) powder sample shown in (Fig. 5), were green, blue, purple, and yellow, indicating the surface morphology of dispersed calcium, phosphor, carbon, and oxygen particles, respectively.

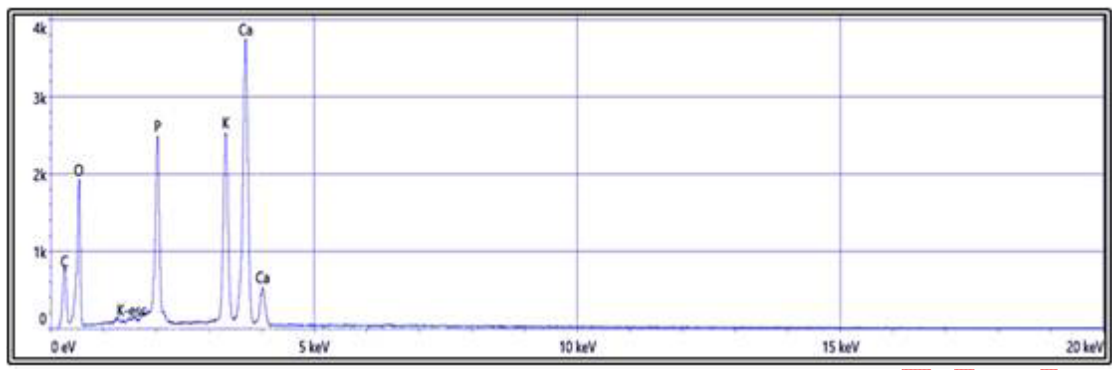


Figure (4): EDX elements spectrum analysis of the fabricated coral shell (HAp) powder.

Table (1) The elements content values of the fabricated coral shell (HAp) powder Sample

Element	Weight %	Atomic %
C	13.4	21.5
O	49.2	59.3
P	8.0	5.0
K	10.2	5.0
Ca	19.2	9.2

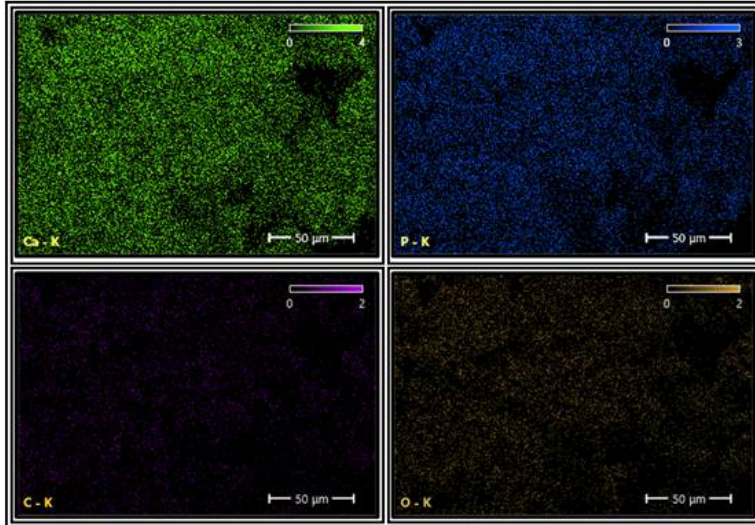


Figure (5): The EDX elemental mapping analysis of the fabricated coral shell (HAp) Powder sample.

#### **FESEM of coral shell hydroxyapatite**

The surface morphology of coral shell hydroxyapatite powder sample heated at 1200 °C for 2h. appear as a spherical particle regularly distributed within the sample with an average diameter (46.9) µm (Fig. 6).

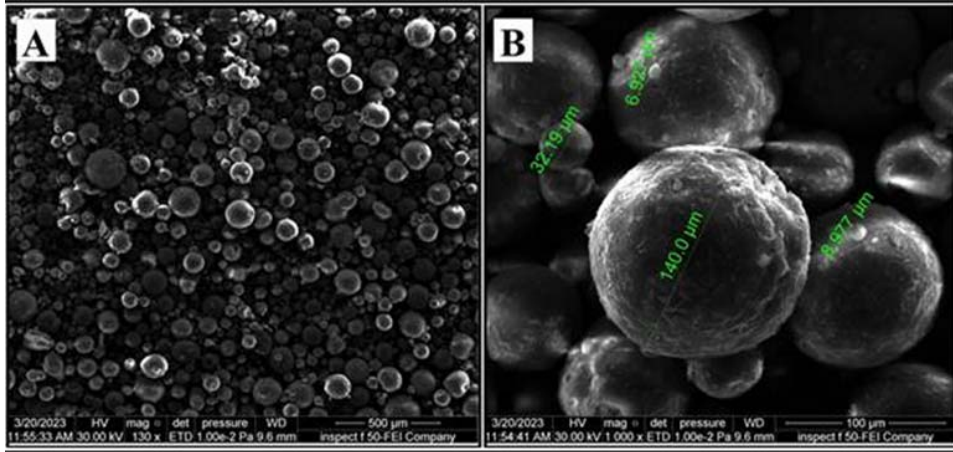


Figure (6): FESEM image of the fabricated coral shell (HAp) powder obtained at the calcination temperature 1200°C for 2h.

### FESEM of the critical size mandibular bone gap defect at 30 days post-surgery

The FESEM images of the defective gap of the mandible bone samples were obtained at 30 days post-surgery shown in (Fig. 7). In the control group, the defective gap appeared partially still open, and the center of the defective gap was filled with a homogenous, smooth matrix surrounded by multiple fibrous tissues, which was the predominant tissue (Fig. 7,A).

In the coral shell (HAp) group, the defective gap appears completely closed and the center of the defect filled with a thick layer of osteoid matrix which appears as a light region beyond many excavations of lamellar bone that faces toward the center of the defective gap (Fig. 7,B).

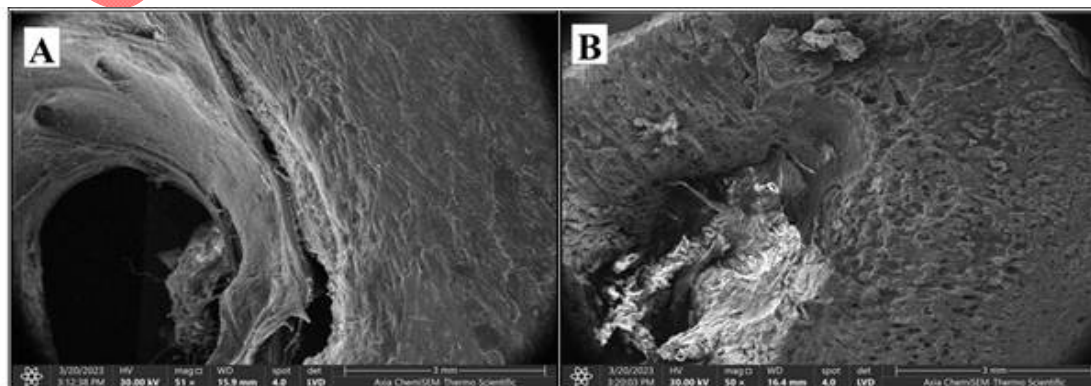


Figure (7): FESEM images of the mandibular bone gap defect at 30 days post-surgery. (A) control group shows that the defective gap still open and surrounded by excessive fibrous tissue. (B) coral shell HA. group shows that the defective gap fill with calcified matrix appears lighter in color and surrounded by lamellar bone.

### **Macroscopical results:**

In the control group, the defective gap at seven days post-surgery appears as a circular gap without any filling tissue, and at 15 days post-surgery, excessive fibrous tissue grows within the defective gap; at the 30 days post-surgery, the excessive fibrous tissue formation within and around the defective gap, without any signs of calcified or cartilaginous tissue formation, and the size of defective gap likely appear in the same diameter. While in the (HAp) group, the defective gap, at seven days post-surgery, seemed to be circular and filled with fibrous tissue. In 15 days post-surgery, the defective gap appears small in diameter, with a small amount of fibrous tissue within the defective area. At 30 days post-surgery, the defective gap appeared very small in size. The defective gap was slightly filled with a small amount of fibrous tissue, with an invasion of new bone formation from the surrounding bone toward the center of the defective area appears as a firm solid white mass, and the edges of the defect become rounded, which face inside the center of the defect. (Fig. 8).

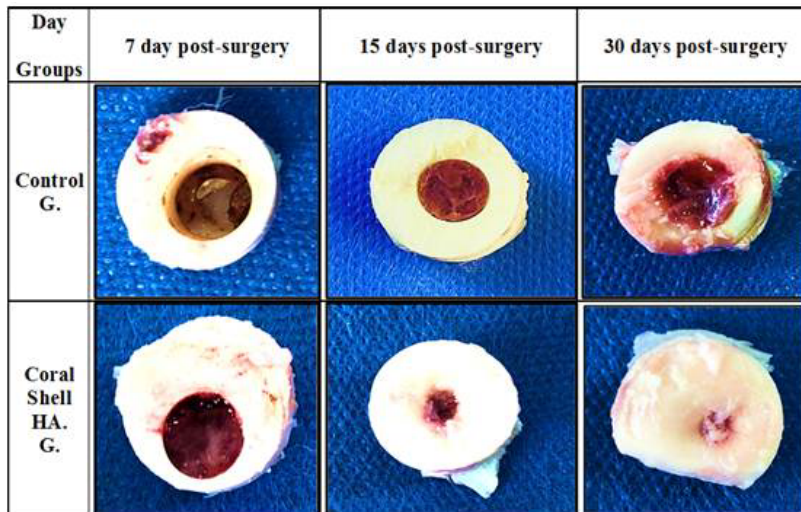


Figure (8): macroscopical findings of the mandibular bone defect in the control and the treated group at 7, 15, and 30 days post-surgery.

### Radiographical results

The radiographic finding in the control group immediately after the operation. The lateral view of the skull represents the induced mandibular bone gap defect which appears as a well-defined circular radiolucent bone defect in the caudal body of the mandible, which seems without trabecular bridging and without any definite significant callus formation, (Fig. 9,A). At 15 days post-surgery, the radiographic findings in the lateral view of the skull showed a well-defined circular radiolucent bone defect at the caudal portion of the mandible, with a relatively slight increase in density which exhibited in the center of the defective area that represented early little callus formation, but without trabecular bridging (Fig. 9,B). At 30 days post-surgery, the radiographic finding indicated a well-defined circular radiolucent bone gap defect in the caudal portion of the mandible, with a partially sclerosed margin and a relative increase in the

opacity only seen as a very fine area of calcification discarded within the center of the defective gap representing a slight developing callus and without trabecular bridging (Fig. 9,C). At 60 days post-surgery, the radiographical finding in the lateral view of the skull still appears as a well-defined circular bone defect in the caudal body of the mandible, which remains open and radiolucent, with a partially sclerosed margin. There was a slight increase in the opacity seen as a small area within the center of the defective gap representing the slightly maturing callus without a complete trabecular bridging (Fig.9,D).

The radiographical finding in the (HAp) group immediately post-surgery, the lateral view of the skull showed the mandibular bone gap defect, which appears as a well-defined circular radiolucent bone gap defect in the caudal body of the mandible. However, it looks clear with no trabecular bridging or definite significant callus formation (Fig. 10,A). At 15 days after the operation, the lateral view of the defective gap shows a well-defined, circular, radiolucent bone gap defect in the caudal body of the mandible, and there was a relative increase in the opacity seen as haziness throughout the defect representing early callus formation with some trabecular bridging (Fig. 10,B). At 30 days post-surgery, the defective gap exhibited slightly definite as a circular gap, with a slightly radiopaque gap defect in the caudal body of the mandible, with a partially sclerosed margin, and there is relatively increased density seen throughout the defect representing developing callus with slightly trabecular bridging (Fig. 10,C). Lastly, at 60 days after the operation, the radiographical findings show partially-defined semicircular, slightly translucent bone gap defect in the caudal body of the mandible, with a sclerosed margin, and there is a relative increase in density seen in the defect representing the maturing callus with a nearly complete trabecular bridging (Fig.10,D).

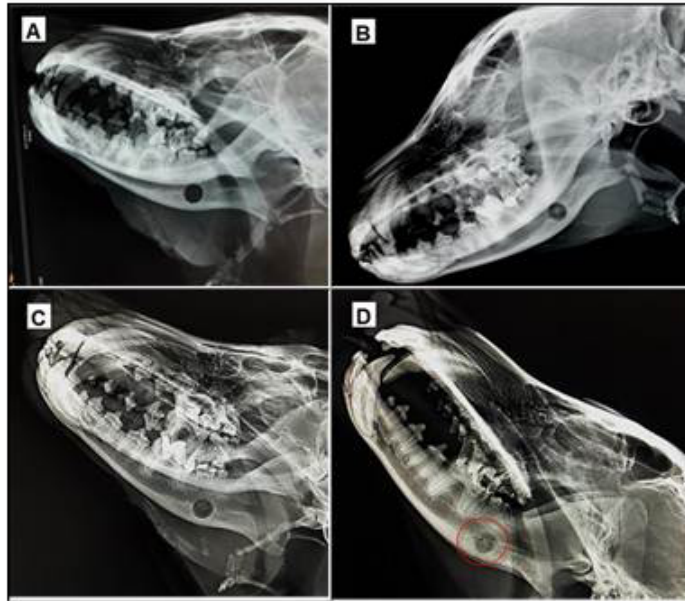


Figure (9): Shows mandibular bone gap defect in the control group. (A) zero time immediately post-surgery. (B) at 15 days post-surgery. (C) at 30 days post-surgery. (D) at 60 days post-surgery.

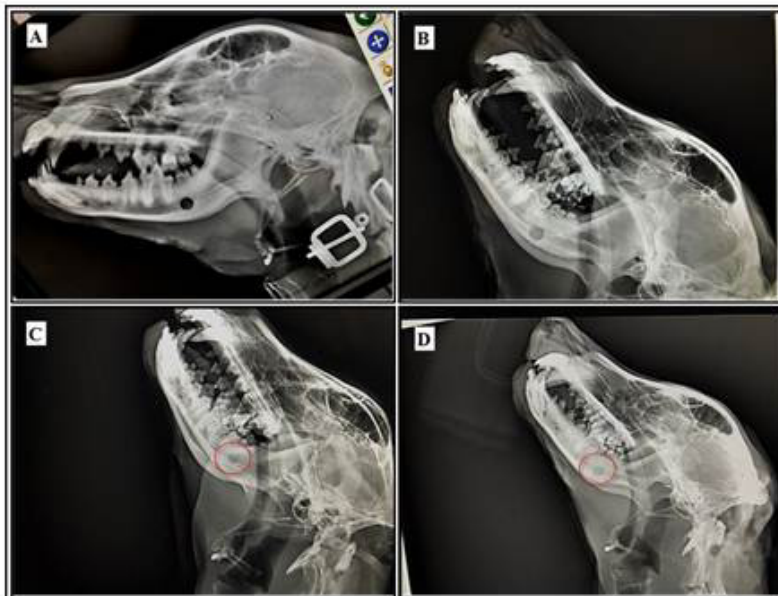


Figure (10): Shows mandibular bone gap defect in (HAp) group. (A) zero time immediately post-surgery. (B) at 15 days post-surgery. (C) at 30 days post-surgery. (D) at 60 days post-surgery.

## Discussion

The mandibular bone has several essential functions in the head and neck. It allows mastication by providing a stable counterpoint to the maxilla and serving as a base for the attachment of the tooth. It also facilitates barking, swallowing, and breathing by maintaining space within the oral cavity and allowing the tongue function.

The FESEM images showed that the coral shell (HAp) were spherical non-aggregation particles with sizes between (6.9-140)  $\mu\text{m}$ . The spherical shape of the (HAp) crystal powder in the Coral shell is dependent on the synthesis method used. It requires prolonged rotation of the solution using a magnetic stirrer to achieve a reaction with a pH of 8. Thus, this result in the slow growth of homogeneously non-agglomerated spherical particles, compared with FESEM images of the quail eggshell Ca(OH) which appear irregular agglomerated particles due to rapid reaction time that do not require PH justification (Zhou and Lee, 2011). Thus, the FESEM images of

fabricated coral shell HAp particles seem more stoichiometric than fabricated quail eggshell  $\text{Ca(OH)}_2$  particles.

The integration behavior of the analyzed FESEM images of current work at 30 days post-implantation seems to be by the process of bone tissue regeneration in the HAp group compared to the control group. In this way, the results came in contact with the previous study mentioned that the biomaterials might support the directed ingrowth of osteoblasts migrating from the native bone tissue neighbored to the defect site (Barbeck et al., 2020). In contrast, (Moshiri et al., 2020) suggested that the shape and the surface morphology responsible for many of their in vivo biological properties and activities .

Clinically mandibular bone defects default for reconstitution due to the complex anatomical structure of the jaw and default for soft tissue repair (Tatara et al., 2019). Most defects of the mandible are mainly acquired and rarely congenital causes, which include cysts, benign and malignant tumors, trauma, and chronic osteomyelitis, loss of teeth (Lim, et al., 2022). The critical size mandibular bone defect described the defect that will not heal spontaneously during the animal's lifetime or using standard treatments (Lim et al., 2022). Dogs have proven to be suitable for studies on the reconstruction of mandibular defects because they easily allow the formation of significant defects with easier surgical access compared to small animals like mice, rats, rabbits, and guinea pigs (Huh et al., 2005). Therefore, we evaluated the healing process of the gap defects macroscopically, radiographically, and morphologically with FESEM imaging to determine the critical size of a mandibular gap defect, along with determining the healing effect of coral shell (HAp) on critically induced mandibular gap defects in dogs.

The results of this study indicated, these bone substitutes have highly biocompatible with the bone tissues because there was no immune rejection or adverse tissues reaction at the site of

the defect. This outcome match with ((Moshiri et al., 2020; Mohammed et al., 2023), whose mentioned that the biomaterials have superior cytocompatibility. Also, Poinern and his colleague mentioned that ceramic biomaterials should not induce any cytotoxicity, immunological rejection, or inflammatory responses from the body (Poinern et al., 2014, Roudana et al.,2017; Mohammed et al., 2023). Also, HAp demonstrates an antimicrobial effect, with activating new bone tissue formation (Halim et al., 2021). Thus decrees the occurrence of bone tissue infection during the filling of the bone defects with fabricated biomaterials.

## **Conclusion**

We concluded that the fabrication (HAp) from natural waste coral shells has practical value in the regeneration of mandibular bone gap as a defect in dogs. Future research should investigate the (HAp) with mesenchymal stem cells to improve the healing process of large-size bone gap defects.

## **Acknowledgments**

The authors is very grateful to the College of Veterinary Medicine, University of Mosul, Iraq, for his support of this study.

## **Conflict of interest**

The manuscript has no conflict of interest.

## **References**

1. Albaroudy, F. M., Alkattan, L. M., and Ismail, H. K. (2022). Histopathological and serological assessment of using rib lamb xenograft reinforced with and without hydroxyapatite nano gel for reconstruction tibial bone defect in dogs. *Iraqi Journal of Veterinary Sciences*, 36, 69-76. [doi.10.33899/IJVS.2022.135366.2473](https://doi.org/10.33899/IJVS.2022.135366.2473)
2. Allawi, A.H, Alkattan, L.M and Al Iraqi, O.M. (2020).The Effect of Autogenous Peritoneal Graft Augmented with Platelets- Plasma Rich Protein on the Healing of Induced Achilles

- Tendon Rupture in Dogs. Iranian Journal Veterinary Medicine ,14:2. [doi: 10.ijvm.2020.291379.1005037](https://doi.org/10.ijvm.2020.291379.1005037)
3. Anvar, A. A., Nowruzi, B., and Afshari, G. (2022). A Review of the Application of Nanoparticles Biosynthesized by Microalgae and Cyanobacteria in Medical and Veterinary Sciences. Iranian Journal of Veterinary Medicine, 17(1): 1-18. <http://dx.doi.org/10.32598/ijvm.17.1.1005309>
  4. Alkattan, L., and Helal, M. (2013). Effects of ketamine-xylazine and propofol-halothane anesthetic protocols on blood gases and some anesthetic parameters in dogs. Veterinary World, 6(2), 95-99. [doi:10.5455/vetworld.2013.95-99](https://doi.org/10.5455/vetworld.2013.95-99)
  5. Atiyah, A. G., Al-Falahi, N. H. R., and Zarraq, G. A. (2021). Synthesis and Characterization of Porous  $\beta$ -Calcium Pyrophosphate Bone Scaffold Derived from Avian Eggshell. Pakistan Journal of Zoology 54( 3), pp. 1439-1442. [doi.org/10.17582/journal.pjz/20200730120707](https://doi.org/10.17582/journal.pjz/20200730120707)
  6. Barbeck, M., Jung, O., Smeets, R., Gosau, M., Schnettler, R., Rider, P., Korzinskas, T. (2020). Implantation of an injectable bone substitute material enables integration following the principles of guided bone regeneration. in vivo, 34(2), 557-568. [doi: 10.21873/invivo.11808](https://doi.org/10.21873/invivo.11808). PMID: 32111754
  7. Cahyaningrum, S., Herdyastuty, N., Devina, B., and Supangat, D. (2018). Synthesis and characterization of hydroxyapatite powder by wet precipitation method. Paper presented at the IOP Conference Series: Materials Science and Engineering [doi. 10.1088/1757-899X/299/1/012039](https://doi.org/10.1088/1757-899X/299/1/012039)
  8. Greene, S., and Thurmon, J. (1988). Xylazine—a review of its pharmacology and use in veterinary medicine. Journal of veterinary pharmacology and therapeutics, 11(4), 295-313. [doi: 10.1111/j.1365-2885.1988.tb00189.x](https://doi.org/10.1111/j.1365-2885.1988.tb00189.x)
  9. Halim, N. A. A., Hussein, M. Z., and Kandar, M. K. (2021). Nanomaterials-upconverted hydroxyapatite for bone tissue engineering and a platform for drug delivery. International journal of Nanomedicine, 16, 6477. [doi: 10.2147/IJN.S298936](https://doi.org/10.2147/IJN.S298936).
  10. Huh, J.-Y., Choi, B.-H., Kim, B.-Y., Lee, S.-H., Zhu, S.-J., and Jung, J.-H. (2005). Critical size defect in the canine mandible. Oral Surgery, Oral Medicine, Oral Pathology, Oral Radiology, and Endodontology, 100(3), 296-301. [doi: 10.1016/j.tripleo.2004.12.015](https://doi.org/10.1016/j.tripleo.2004.12.015). PMID: 16122656
  11. Kaneko, A., Marukawa, E., and Harada, H. (2020). Hydroxyapatite nanoparticles as injectable bone substitute material in a vertical bone augmentation model. in vivo, 34(3), 1053-1061. doi: [10.21873/invivo.11875](https://doi.org/10.21873/invivo.11875) PMID: [32354892](https://pubmed.ncbi.nlm.nih.gov/32354892/)
  12. Khan, S. R., Jamil, S., Rashid, H., Ali, S., Khan, S. A., and Janjua, M. R. S. A. (2019). Agar and egg shell derived calcium carbonate and calcium hydroxide nanoparticles: Synthesis, characterization and applications. Chemical Physics Letters, 732, 136662.

13. Lim, H.-K., Choi, Y.-J., Choi, W.-C., Song, I.-S., and Lee, U.-L. (2022). Reconstruction of maxillofacial bone defects using patient-specific long-lasting titanium implants. *Scientific Reports*, 12(1), 7538. doi.org/10.1038/s41598-022-11200-0.
14. Mohammed, F.M., Alkattan, L.M, Ahmed, M.S. and Thanoon, M.G.( 2023). Evaluation the effect of high and low viscosity Nano-hydroxylapatite gel in repairing of an induced critical-size tibial bone defect in dogs: Radiological study. *Journal of Applied Veterinary Sciences*, 8 (3): 105-110. doi: 10.21608/JAVS.2023.215990.1239.
15. Moshiri, A., Maroof, N. T., and Sharifi, A. M. (2020). Role of organic and ceramic biomaterials on bone healing and regeneration: An experimental study with significant value in translational tissue engineering and regenerative medicine. *Iranian Journal of Basic Medical Sciences*, 23(11), 1426. doi:10.22038/ijbms.2020.46228.10707. PMID: 33235700
16. Paré, A., Bossard, A., Laure, B., Weiss, P., Gauthier, O., and Corre, P. (2019). Reconstruction of segmental mandibular defects: Current procedures and perspectives. *Laryngoscope Investigative Otolaryngology*, 4(6), 587-596. doi.org/10.1002/lio2.325.
17. Pina, S., Rebelo, R., Correló, V. M., Oliveira, J. M., and Reis, R. L. (2018). Bioceramics for Osteochondral Tissue Engineering and Regeneration. *Advance Experimental Med Biol*, 1058, 53-75. doi:10.1007/978-3-319-76711-6\_3
18. Pina, S., Vieira, S., Rego, P., Torres, P., da Cruz E Silva, O., da Cruz E Silva, E., and Ferreira, J. (2010). Biological responses of brushite-forming Zn-and ZnSr-substituted beta-tricalcium phosphate bone cements. *European Cell Mater*, 20, 162-177. doi: 10.22203/ecm.v020a14. PMID: 20821372
19. Poinern, G. E. J., Brundavanam, R. K., Thi Le, X., Nicholls, P. K., Cake, M. A., and Fawcett, D. (2014). The synthesis, characterisation and in vivo study of a bioceramic for potential tissue regeneration applications. *Scientific Reports*, 4(1), 6235. doi: 10.1038/srep06235. PMID: 25168046
20. Shafiei-Sarvestani, Z., Oryan, A., Bigham, A. S., and Meimandi-Parizi, A. (2012). The effect of hydroxyapatite-hPRP, and coral-hPRP on bone healing in rabbits: radiological, biomechanical, macroscopic and histopathologic evaluation. *Int J Surg*, 10(2), 96-101. doi:10.1016/j.ijsu.2011.12.010
21. Roudana, M. A.; Ramesha, S.; Niakanb, A.; Wonga, Y. H.; Zavareha, M. A.; Chandranc, H. and Sutharsinif, U. Thermal phase stability and properties of hydroxyapatite derived from bio-waste eggshells. *Journal of Ceramic Processing Research*, 2017;18(1): 69-72. https://www.researchgate.net/publication/316062556

22. Szcześ, A., Hołysz, L., and Chibowski, E. (2017). Synthesis of hydroxyapatite for biomedical applications. *Advances in colloid and interface science*, 249, 321-330. [doi: 10.1016/j.cis.2017.04.007](https://doi.org/10.1016/j.cis.2017.04.007). PMID: 28457501
23. Tataru, A. M., Koons, G. L., Watson, E., Piepergerdes, T. C., Shah, S. R., Smith, B. T., Mikos, A. G. (2019). Biomaterials-aided mandibular reconstruction using in vivo bioreactors. *Proc Natl Acad Sci U S A*, 116(14), 6954-6963. [doi:10.1073/pnas.1819246116](https://doi.org/10.1073/pnas.1819246116).
24. Yal Beiranvand, S., Nourani, H., Kazemi Mehrjerdi, H. (2022). Fabrication of Platelet-Rich Fibrin-Coated Polycaprolactone/Hydroxyapatite (PCL-HA/PRF) 3D Printed Scaffolds for Bone Tissue Engineering. *Iranian Journal of Veterinary Medicine*, 16(4), 400-413. [doi:10.22059/IJVM.2022.335899.1005219](https://doi.org/10.22059/IJVM.2022.335899.1005219)
25. Zhang, H., Zhou, Y., Yu, N., Ma, H., Wang, K., Liu, J., He, Y. (2019). Construction of vascularized tissue-engineered bone with polylysine-modified coral hydroxyapatite and a double cell-sheet complex to repair a large radius bone defect in rabbits. *Acta biomaterialia*, 91, 82-98. [doi: 10.1016/j.actbio.2019.04.024](https://doi.org/10.1016/j.actbio.2019.04.024). PMID: 30986527.
26. Zhou, H., and Lee, J. (2011). Nanoscale hydroxyapatite particles for bone tissue engineering. *Acta biomaterialia*, 7(7), 2769-2781. [doi.org/10.1016/j.actbio.2011.03.019](https://doi.org/10.1016/j.actbio.2011.03.019)